

# Current-controlled dynamic magnonic crystal

A. V. Chumak, T. Neumann, A. A. Serga, and B. Hillebrands  
Fachbereich Physik and Forschungszentrum OPTIMAS,  
Technische Universität Kaiserslautern, 67663 Kaiserslautern, Germany

M. P. Kostylev

School of Physics, University of Western Australia, Crawley, Western Australia 6009, Australia  
(Dated: February 21, 2024)

We demonstrate a current-controlled, dynamic magnonic crystal. It consists of a ferrite film whose internal magnetic field exhibits a periodic, cosine-like variation. The field modulation is created by a direct current flowing through an array of parallel wires placed on top of a spin-wave waveguide. A single, pronounced rejection band in the spin-wave transmission characteristics is formed due to spin-wave scattering from the inhomogeneous magnetic field. With increasing current the rejection band depth and its width increase strongly. The magnonic crystal allows a fast control of its operational characteristics via the applied direct current. Simulations confirm the experimental results.

PACS numbers: 75.50.Gg, 75.30.Ds, 75.40.Gb

Spin waves in magnetic materials attract special attention because of their potential application as information units in signal processing devices. Digital spin wave logic devices [1, 2] as well as devices for analogous signal processing [3, 4, 5] can be fabricated based on spin waves. It has been shown that the spin-wave relaxation, one of the main obstacles for spin-wave application, can be overcome by means of parametric amplification [5, 6].

The study of spin waves in magnetic materials is also interesting from a fundamental point of view. The interaction of the numerous existing spin-wave modes in ferromagnetic samples [7] as well as nonlinear effects such as soliton formation [8, 9] are just some examples.

Magnonic crystals, which are defined as artificial media with a spatially periodic variation of some of their magnetic parameters, constitute a research field which connects fundamental physics with application [10, 11, 12, 13, 14]. They are the analogue of photonic crystals which operate with light. The spectra of spin-wave excitations in such structures are considerably modified compared to uniform media and exhibit features such as full band gaps where spin waves are not allowed to propagate.

Promising functionalities arise by taking advantage of the dynamic controllability and by potentially changing the characteristics of the magnonic crystal faster than the spin-wave relaxation time: even the simple possibility to "switch" a periodical inhomogeneity on and off immediately offers a method to trap and release a spin wave packet. This can be exploited for instance in information storage.

Here, we present a first realization of such a dynamic magnonic crystal. It is based on spin-wave propagation in an yttrium iron garnet (YIG) film placed in a periodically varying, dynamically controllable magnetic field. The magnetic field is created by the superposition of a

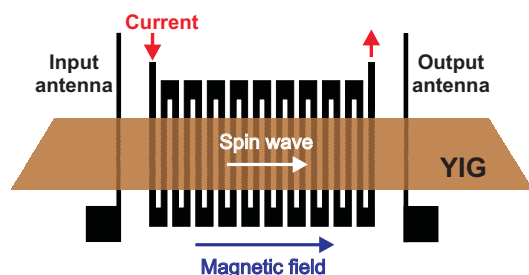


FIG. 1: (Color online) Sketch of the magnonic crystal structure used in the experiments.

spatially homogeneous bias magnetic field with the localized Oersted fields of current carrying wires which are placed in an array layout close to the YIG film surface [15]. By controlling the direct current in the wires the field modulation is adjusted and the spin-wave transmission is changed from full transmission for no applied current to a transmission showing a distinct, 30 MHz-wide stop band for an applied current of 1.25 A. The dynamic controllability constitutes a major difference to previous realizations of magnonic crystals with a periodically varying magnetic field [6].

Previous studies focused on the interaction of propagating spin-wave packets with the Oersted field of a single current carrying wire or a set of two wires at most [17, 18, 19, 20, 21]. It was shown that the spin-wave transmission can be effectively changed by varying the value of the direct current. However, the appearance of a pronounced frequency stop-band, for which spin-wave transmission is prohibited (while it remains almost unaffected outside the band), is only observed for larger wire numbers.

A sketch of the experimental section is shown in Fig. 1. It consisted of a 5 nm-thick YIG film which was epitaxially grown on a gallium gadolinium substrate. A bias magnetic field of  $4.176 \text{ A m}^{-1}$  was applied along the

arXiv:0904.0332v1 [cond-mat.other] 2 Apr 2009

Electronic address: chumak@physik.uni-kl.de

YIG waveguide so that the conditions for the propagation of backward volume magnetostatic waves (BVM SWs) are given.

To achieve a periodic modulation of the magnetic field an array of connected, parallel wires was designed. The wire structure was patterned by means of photolithography on an aluminum nitride substrate with high thermal conductivity in order to avoid heating. The structure consists of 40 wires of 75  $\mu\text{m}$  width with a 75  $\mu\text{m}$  spacing.

The wire array was placed above the YIG film in such a way that the wires ran perpendicularly to the spin-wave waveguide. Thus, the magnetic Oersted field produced by each of the current carrying wire segments is oriented in first approximation parallel to the bias magnetic field.

In the experiment the individual wires were connected to form a meander structure [15] where the current in neighboring wires flows in opposite directions (see Fig. 1). Thus, a magnonic crystal with a lattice constant  $a = 300 \mu\text{m}$  and 20 repetitions was fabricated.

Another possible configuration would have all currents flowing in the same directions ("multi-strip structure") so that for all wires the Oersted fields have identical orientation. This is an advantage since our previous studies have shown the existence of two physically different regimes for the different field orientations: When the Oersted field decreases the internal field one implements the spin-wave tunneling regime [18]. When the internal field is locally increased the conditions for resonant spin-wave scattering [19] can be fulfilled for which the spin-wave transmission depends non-monotonically on the applied current and exhibits a strong frequency dependence [20].

However, the meander structure has important advantages: (i) It produces a much stronger periodic modulation because the in-plane components of the Oersted fields for neighbouring wires are oriented in opposite directions. (ii) It ensures that the magnetic field averaged over the structure remains constant for any current magnitude.

Two microstrip antennas were placed, one in front and another one behind the wire structure (see Fig. 1) in order to excite and detect BVM SWs. A network analyzer connected to the input and output antennas was used to measure the spin-wave transmission characteristics.

In order to minimize the electromagnetic coupling between the current carrying wire segments and the spin waves, a 100  $\mu\text{m}$  thick  $\text{SiO}_2$  spacer was placed between the YIG film and the wire structure. Note, that the spin-wave dipole field decays exponentially with the distance from the film surface while the Oersted field around the wires scales with the inverse distance between the wire and the film surface. The distance of 100 microns between the wire array and the film surface proved to be large enough to avoid any disturbance of the spin-wave propagation by the meander conductor, but still small enough to ensure an efficient modulation of the magnetic field in the film by the current field.

Experimental results are shown in Fig. 2. The dotted curves in the panels show the transmission characteristics without direct current applied to the wires. They

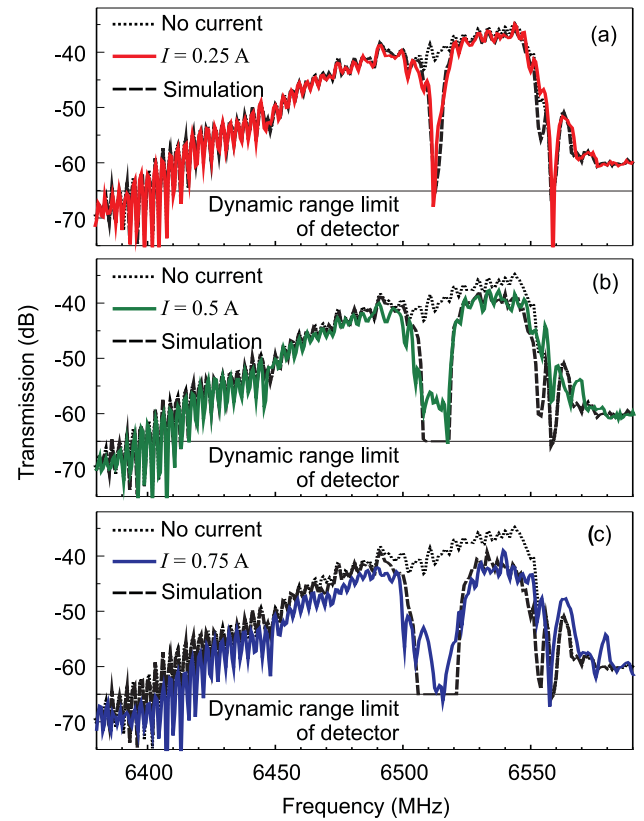


FIG. 2: (Color online) Spin-wave transmission characteristics in a uniform magnetic field (dotted curves) and in a magnetic field which is periodically modulated by the current  $I$  applied to the wires (solid curves). The dashed curves are calculated as the product of the experimentally observed transmission in a uniform field with the transmission coefficient obtained from the numerical simulations (where in addition the limited dynamic range of the experimental setup is taken into account).

are typical for BVM SWs, limited by the ferromagnetic resonance frequency towards high frequencies and by the antenna excitation efficiency from the opposite side. The minimal transmission loss of about 35 dB is determined by the spin-wave excitation/reception efficiency of the microwave antennas and by the spin-wave relaxation parameter of the ferrite film.

Figure 2 (a) shows that the application of a current  $I = 0.25 \text{ A}$  to the structure results in the appearance of a pronounced rejection band at a frequency  $f_1 = 6510 \text{ MHz}$  where the transmission of spin waves is prohibited. The rejection band already appears for a current as small as 80 mA. With an increase in the current the rejection band depth increases rapidly and for 0.25 A it reaches the dynamic range of the experimental setup which is limited mainly by the direct electromagnetic leakage between the microstrip antennas. A further increase in the current applied to the wires results in a pronounced broadening of the rejection band (see Fig. 2 (b) and Fig. 2 (c)).

We emphasize one particularly interesting feature of

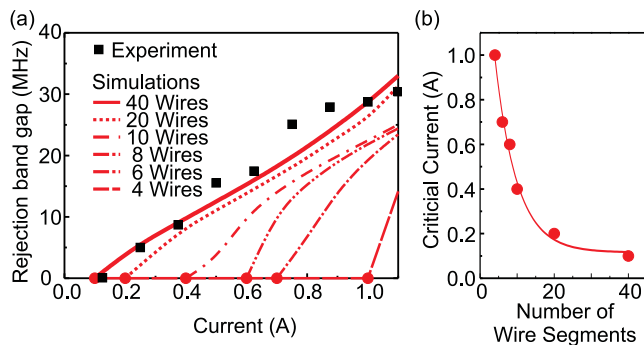


FIG. 3: (Color online) (a) Experimentally obtained width of the first rejection band as a function of the current applied to the wires. The lines and filled circles represent the results of numerical simulations. (b) Calculated critical current for which a band gap with a suppression of 90% is obtained for different numbers of parallel wire segments. The line indicates a fit with a decaying exponential function.

the magnonic crystal presented here. Practically only one rejection band is formed. This is not true for magnonic crystals consisting of an array of grooves on the YIG film surface [13] where multiple rejection bands are formed. As shown by our calculations, for the magnonic crystal studied here the spatially periodic modulation of the magnetic field is close to cosinusoidal. For an ideal harmonic variation only one rejection band should exist since the reflection amplitude is proportional to the Fourier component of the inhomogeneity profile corresponding to twice the spin-wave wave vector as seen from Eq. (6) in [19].

The presence of only one rejection band is an advantage for applications in a microwave filter device. Another positive aspect of the presented dynamic crystal is that practically no losses occur for frequencies outside the induced stop band with increasing current (see Fig. 2 (c)). In the groove-structure-based magnonic crystal [13] such undesired parasitic increase of losses in the transmission bands was observed for larger groove depths.

In order to investigate the dynamic properties of the magnonic crystal additional experiments with a pulsed direct current supplied to the meander structure were performed. The microwave frequency which was applied to the input antenna to excite the spin-wave signal was chosen inside the rejection band ( $f = 6.51$  GHz). The direct current supplied to the meander structure was pulsed with a duration of 50 ns and a strength of 0.5 A. The obtained results show that the spin-wave transmission can be dynamically turned on and off with a transition time for the magnonic crystal of approximately 50 ns.

The measured rejection band width as a function of the applied current is shown in Fig. 3 (a). It was measured for the first rejection band at the power level where the spin-wave intensity decreases to one tenth, i.e. 10 dB, of its value. One can see that the band width can be

tuned from 5 MHz for 125 mA current to 31 MHz for 1.25 A and exhibits a linear behavior with respect to the applied current. The possibility of a dynamic control of the rejection band width seems to be promising for the design of a dynamic stop-band microwave filter. The center frequency of the rejection band can be controlled by means of an applied magnetic field.

The experimental results were confirmed by numerical simulations. We used a 1-dimensional approach, in which the dipole field was expressed via a Green's function and the magnetic field was averaged over the film thickness. Details on the model can be found in [19]. The obtained frequency-dependent transmission curves show a single, well pronounced stop-band for low currents which coincides well with the experiment (see Fig. 2). The calculated rejection efficiency, given by the depth of the stop band, reached up to 150 dB which exceeds the dynamic range in the experiment greatly.

Two effects are observed if the number of parallel wire segments in the simulation is decreased: Firstly, the achieved stop-band width for a given current decreases slightly. Secondly, the rejection efficiency decreases dramatically. As a consequence, the desired signal suppression (e.g. one tenth of the transmission for no applied current) is only reached for higher currents which results in the behavior of the rejection band gap width shown in Fig. 3 (a). Figure 3 (b) summarizes the calculated dependence of the critical current necessary to obtain a 10 dB signal suppression on the number of parallel wire segments. As can be seen a larger number of wires exponentially reduces the critical current which has a particularly pronounced effect on the current if the number of wires is smaller than 20.

In conclusion, we presented a current-controlled magnonic crystal whose operational characteristics can be tuned dynamically within a transition time of 50 ns. The spatially periodic Oersted field of a meander conductor located in the vicinity of YIG film surface results in a pronounced modification of spin wave dispersion which leads to the appearance of spin-wave rejection bands. The width of the main rejection band varies linearly with the magnitude of applied direct current and can be tuned in the range from 5 MHz to 30 MHz. Numerical simulations are in good qualitative agreement with the experiment. Overall, the presented dynamic magnonic crystal is promising for the investigation of linear and nonlinear spin-wave dynamics and can be used as a dynamically controlled microwave stop-band filter.

Financial support by the DFG project SE 1771/1-1, the Max Planck Graduate School of Excellence, the Australian Research Council, and the University of Western Australia is acknowledged. Special acknowledgments go to the Nano+Bio Center, TU Kaiserslautern. T. Neumann would like to thank especially Robert L. Stamps and the University of Western Australia for their assistance during his research stay.

- 
- [1] T. Schneider, A. A. Serga, B. Leven, B. Hillebrands, R. L. Stamps, and M. P. Kostylev, *Appl. Phys. Lett.* 92, 022505 (2008).
- [2] K. Lee and S. Kim, *J. Appl. Phys.* 104, 053909 (2008).
- [3] J. D. Adam, *Proc. IEEE* 76, 159 (1988).
- [4] Yu. V. Kobljanskyj, G. A. Melkov, A. A. Serga, V. S. Tiberkevich, and A. N. Slavin, *Appl. Phys. Lett.* 81, 1645 (2002).
- [5] A. A. Serga, A. V. Chumak, A. Andre, G. A. Melkov, A. N. Slavin, S. O. Demokritov, and B. Hillebrands, *Phys. Rev. Lett.* 99, 227202 (2007).
- [6] E. Schlömann, J. J. Green, and U. Milano, *J. Appl. Phys.* 31, 386S (1960).
- [7] B. A. Kalinikos and A. N. Slavin, *J. Phys. C* 19, 7013 (1986).
- [8] B. A. Kalinikos, N. G. Kovshikov, and A. N. Slavin, *JETP Lett.* 38, 413 (1983).
- [9] S. O. Demokritov, A. A. Serga, V. E. Demidov, B. Hillebrands, M. P. Kostylev, and B. A. Kalinikos, *Nature* 426, 159 (2003).
- [10] K. W. Reed, J. M. Owens, and R. L. Carter, *Circ. Syst. Signal Process.* 4, 157 (1985).
- [11] Yu. V. Gulyaev, S. A. Nikitov, L. V. Zhivotovskii, A. A. Klimov, Ph. Tailhades, L. P. Resnanes, C. Bonningue, C. S. Tsai, S. L. Vysotskii, and Yu. A. Filimonov, *JETP Letters* 77, 567 (2003).
- [12] M. P. Kostylev, P. Schrader, R. L. Stamps, G. G ubbiotti, G. Carloti, A. O. Adeyeye, S. Gookup, and N. Singh, *Appl. Phys. Lett.* 92, 132504 (2008).
- [13] A. V. Chumak, A. A. Serga, B. Hillebrands, and M. P. Kostylev, *Appl. Phys. Lett.* 93, 022508 (2008).
- [14] Z. K. Wang, V. L. Zhang, H. S. Lin, S. C. Ng, M. H. Kuok, S. Jain, and A. O. Adeyeye, *Appl. Phys. Lett.* 94, 083112 (2009).
- [15] A. N. Miasoedov and Y. K. Fetisov, *Sov. Phys. Tech. Phys.* 34, 666 (1989).
- [16] A. V. Voronenko, S. V. Genus, and V. D. Haritonov, *Sov. Phys. J.* 31, 76 (1988).
- [17] A. A. Serga, T. Neumann, A. V. Chumak, and B. Hillebrands, *Appl. Phys. Lett.* 94, 112501 (2009).
- [18] S. O. Demokritov, A. A. Serga, A. Andre, V. E. Demidov, M. P. Kostylev, and B. Hillebrands, *Phys. Rev. Lett.* 93, 047201 (2004).
- [19] M. P. Kostylev, A. A. Serga, T. Schneider, T. Neumann, B. Leven, B. Hillebrands, and R. L. Stamps, *Phys. Rev. B* 76, 184419 (2007).
- [20] T. Neumann, A. A. Serga, B. Hillebrands, and M. P. Kostylev, *Appl. Phys. Lett.* 94, 042503 (2009).
- [21] U. H. Hansen, M. G atzen, V. E. Demidov, and S. O. Demokritov, *Phys. Rev. Lett.* 99, 127204 (2007).